J Clust Sci (2011) 22:673–692
DOI 10.1007/s10876-011-0414-2

ORIGINAL PAPER

EPR Study of Electronic Structure of $[CoF_6]^{3-}$and $B_{18}N_{18}$ Nano Ring Field Effects on Octahedral Complex

M. Monajjemi · M. Khaleghian

Received: 5 August 2011 / Published online: 27 September 2011

Abstract Density functional theory calculations (DFT), as well as hybrid methods (B3LYP) for $B_{18}N_{18}$-$[CoF_6]^{3-}$ complex have been carried out to study the non-bonded interaction. The geometry of the $B_{18}N_{18}$ has been optimized at B3LYP method with EPR-II basis set and geometry of the $[CoF_6]^{3-}$ have been optimized at B3LYP method with Def2-TZVP basis set and Stuttgart RSC 1997 Effective Core Potential. The electromagnetic interactions of the $[CoF_6]^{3-}$ molecule embedded in the $B_{18}N_{18}$ Nano ring have been investigated at B3LYP and total atomic charges, spin densities, dipole moment and isotropic Fermi coupling constants parameters in different loops and bonds of the $B_{18}N_{18}$-$[CoF_6]^{3-}$ system have been calculated. Also NBO analysis such as electronic delocalization between donor and acceptor bonds has been studied by DFT method. Then we have been investigated the lowest unoccupied molecular orbital (LUMO) and the highest occupied molecular orbital (HOMO) for the lowest energy have been derived to estimate the structural stability of the $B_{18}N_{18}$-$[CoF_6]^{3-}$ system, and the coefficients of s, p and d orbitals of Co-F bonds involved in $B_{18}N_{18}$-$[CoF_6]^{3-}$.Thus, hybridization of Co and F atoms can be distinguished based on these NBO data. The Gaussian quantum chemistry package is used for all calculations.

Keywords DFT · Dipole moment · ECP · EPR-II basis set · HOMO · LUMO · NICS · LCAO · Hyperfine properties

Abbreviations

DFT	Density functional theory
EPR	Electron paramagnetic resonance

M. Monajjemi (✉)
Department of Chemistry, Science and Research Branch, Islamic Azad University, Tehran, Iran
e-mail: m_monajjemi@yahoo.com

M. Khaleghian
Science and Research Branch, Islamic Azad University, Tehran, Iran

HOMOL	Highest occupied molecular orbital
LUMO	Lowest unoccupied molecular orbital
ECP	Effective core potential
NICS	Nuclear independent chemical shift
LCAO	Linear combination of atomic orbitals

Introduction

There has been a significant interest in experimental studies of B_nN_m clusters that can be found in the literature, and several research groups have described the production of boron nitride-based nano-structures [1–6]. Recently, various cages and $(BN)_n$ cubes have been synthesized [7–12], BN polyhedral have also been successfully synthesized by reaction of BCl_3 with NH_3 in a laser beam [13, 14]. There are mainly two structural classes for $(BN)_n$ cages [10, 15]. One is constructed from alternate BN units and governed by an isolated square rule [16, 17], which is the counterpart of the isolated hexagonal rule of carbon fullerenes. Another class is of fullerene-like structures, based on combination of 5- and 6-membered rings, with the existence of N–N and B–B bonds. In addition to the theoretical predictions for the structures, physical properties of such molecules of $B_{24}C_{12}N_{24}$ molecule [15] and the $B_{12}N_{12}$, $B_{16}N_{16}$ and $B_{28}N_{28}$ molecules, the experimental synthesis and various spectrometer are needed for the final confirmation of their stability for structures [16–19]. However, there is basically no experimental information on the B_nN_m cluster thermo chemistry, though some information for small aggregates can be derived from ab initio calculations [20–23]. We have employed single wall borane nitride nanotube (SWBNNT) from kind MWNT = 1, as an armchair nanotubes (n, m) with chirality $n = 5$, $m = 5$ and the tube length was 3 Å. The schematics of the generation of our considered nanotube through folding a section of a graphene sheet and the optimized structure of $B_{18}N_{18}$ are displayed in the Scheme, where $C = n\,a_1 + m\,a_2 = (n,m)$, a_1 and a_2 are the primitive lattice vectors of the graphene and n, m are integers [24, 25]. Molecular orbital theory was developed, in the years after valence bond theory had been established (1927), primarily through the efforts of Friedrich Hund, Robert Mulliken, John C. Slater, and John Lennard-Jones. The first accurate calculation of a molecular orbital wave function was that made by Charles Coulson in 1938 on the hydrogen molecule. By 1950, molecular orbitals were completely defined as wave functions of the self-consistent field Hamiltonian and it was at this point that molecular orbital theory became fully rigorous and consistent[26]. This rigorous approach is known as the Hartree–Fock method for molecules although it had its origins in calculations on atoms. This led to the development of many ab initio quantum chemistry methods. Parallel to this rigorous development, molecular orbital theory was applied in an approximate manner using some empirically derived parameters in methods now known as semi-empirical quantum chemistry methods [27]. The aim of the present study was the investigation of the electrostatic interactions within the $B_{18}N_{18}$-$[CoF_6]^{3-}$ system. For further investigation about electrostatic interactions, the

quantum mechanical atomic charges caused by the asymmetric distribution of electrons in chemical bonds play an important role in simulations of intermolecular forces and condensed phase properties and they are also often used for a qualitative understanding of the structural aspects and mutual electrostatic interaction of two molecules [28]. We report the non-bonded interaction [29, 30] of the $[CoF_6]^{3-}$ embedded in $B_{18}N_{18}$ nano ring. In chemistry, octahedral molecular geometry describes the shape of compounds where in six atoms or groups of atoms or ligands are symmetrically arranged around a central atom, defining the vertices of an octahedron. Stability structure of $[CoF_6]^{3-}$ under the different loops and bonds of $B_{18}N_{18}$ nano ring have been calculated. For further structural information, the lowest unoccupied molecular orbital and the highest occupied molecular orbital differences, namely band gaps and the hybrids on atom have been reported to explore the ability of the $[CoF_6]^{3-}$ to create a stable $B_{18}N_{18}$-$[CoF_6]^{3-}$ system.

Computational Details

In chemistry, molecular orbital theory is a method for determining molecular structure in which electrons are not assigned to individual bonds between atoms, but are treated as moving under the influence of the nuclei in the whole molecule. In this theory, each molecule has a set of molecular orbitals, in which it is assumed that the molecular orbital wave function ψ_j may be written as a simple weighted sum of the n constituent atomic orbitals χ_i, according to the following equation:

$$\Psi_j = \sum_{i=1}^{n} c_{ij}\chi_i \tag{1}$$

The c_{ij} coefficients may be determined numerically by substitution of this equation into the Schrodinger equation and application of the variational principle. This method is called the linear combination of atomic orbitals approximation and is used in computational chemistry. Molecular orbital (MO) theory uses a linear combination of atomic orbitals (LCAO) to represent molecular orbitals involving the whole molecule. These are often divided into bonding orbitals (σ, π), anti-bonding orbitals (σ^*, π^*), and non-bonding orbitals or lone pairs orbitals (n), that σ^*—almost never occupied in the ground state, π^*—very rarely occupied in the ground state, n—lone pairs, π—always occupied in compounds with multiple bonds, σ—at least one occupied in all molecules. The $[CoF_6]^{3-}$ complex including octahedral symmetric Co (III) coordination compounds and six π-donor ligands. The geometry of the $[CoF_6]^{3-}$ have been optimized at B3LYP method with Def2-TZVP basis set and Stuttgart RSC 1997 effective core potential (ECP). ECP operators are sums of products of polynomial radial functions, Gaussian radial functions and angular momentum projection operators. ECP input therefore specifies which potential to use on each atomic center, and then includes a collection of triplets of: (coefficient, power of R, exponent) for each potential for each term in each angular momentum of the ECP. Since only the first few angular momentum components have different terms, the potential is expressed as (1) terms

for the general case, typically d or f and higher projection, and (2) the extra terms for each special angular momentum. Thus, for an LP-31G potential, which includes special s and p projected terms, the input includes the general (d and higher) term, the s–d term (i.e., what to add to the general term to make the s component) and the p–d term. The geometry of the $B_{18}N_{18}$ ring and $[CoF_6]^{3-}$ complex have been optimized by Becke's hybrid three-parameter exchange functional and the non-local correlation functional of Lee, Yang and Parr (B3LYP) method [31, 32] with EPR-II basis sets of Barone [33] using ab initio GAUSSIAN quantum chemical package [34]. EPR-II is a double zeta basis set with a single set of polarization functions and an enhanced s part: (6,1) [8, 33] for H and (10,5,1) [10, 33, 35] for B to F. Also in this case the s-part is improved to better describe the nuclear region: (6,2) [35, 36] for H and [11, 14, 33, 35] for B to F. Vibrational frequencies have been calculated at the level of B3LYP/EPR-II theory to verify that the geometry was a real minimum without any imaginary frequency and analyze the thermochemical functions including enthalpies and Gibbs free energies [37]. The natural bond orbital (NBO) analysis [38, 39] has also been applied. To study the intermolecular orbital interactions in the complexes [40, 41]. Also, the isotropic Fermi [42] coupling which depends on the direct transfer of electron spin to the s orbital of a proton, total atomic charges and spin densities of $[CoF_6]^{3-}$ in different loops and bonds of $B_{18}N_{18}$-$[CoF_6]^{3-}$ system have been evaluated with EPR-II and Def2-TZVP basis sets and Stuttgart RSC 1997 ECP to get a deeper insight about the non-bonded electrostatic interaction between $[CoF_6]^{3-}$ and the $B_{18}N_{18}$ ring.

Result and Discussion

The $[CoF_6]^{3-}$ complex including octahedral symmetric Co (III) coordination compounds and six π-donor ligands. The geometry of the $[CoF_6]^{3-}$ have been optimized at B3LYP method with Def2-TZVP basis set and Stuttgart RSC 1997 ECP. Optimized parameters of $[CoF_6]^{3-}$ such as bond lengths and bond angles have been reported in Table 1. We can view the Co-F(4) and Co-F(5) bond lengths are less than other bond lengths, because the octahedral symmetric Co (III) coordination compounds and six π-donor ligands are High-spin d^6 electronic configuration ($S = 2$) exhibit the Elongation Jahn–Teller distortion.

In accordance with the occupancy values of metal Co (III) in Table 2, it was elaborated that $3d_{xz}$ orbital consists of two electrons and has the least value of energy. The other d orbitals are single and 4S orbital has no electron. Also, in accordance with the occupancy and energy values for 6 ligands of π-donor in atoms F(7)—F(2) it was demonstrated that three non bonding electron pairs of F are in 2 s and two 2p orbitals that have higher energy levels. For instance, in F(2), $2p_z$ is single and has a lower energy level; $2p_x$ and $2p_y$ that have higher energy levels and are nearer to the metal d orbitals in energy, interfere to make molecular π orbitals and 2 s orbitals interfere to make the σ molecular orbitals. In addition, related to Table 2 data, atoms F(4)–F(5), F(3)–F(6) and F(2)–F(7) that are in one direction related to Co (III), are the same in occupancy and energy levels (Fig. 1).The different energy levels of metal-ligands bonding in $[CoF_6]^{3-}$ complex have been

Table 1 Optimized parameters of octahedral symmetric Co (III) coordination compounds and six π-donor ligands

Compound	Bond ID	Bond length	Bond angle
$[CoF_6]^{3-}$	Co(1)–F(2)	2.065	–
	Co(1)–F(3)	2.065	–
	Co(1)–F(4)	1.945	–
	Co(1)–F(5)	1.945	–
	Co(1)–F(6)	2.065	–
	Co(1)–F(7)	2.065	–
	F(2)–Co(1)–F(3)	–	90.000
	F(2)–Co(1)–F(4)	–	90.010
	F(2)–Co(1)–F(5)	–	89.990
	F(2)–Co(1)–F(6)	–	90.000
	F(2)–Co(1)–F(7)	–	179.981
	F(3)–Co(1)–F(4)	–	89.986
	F(3)–Co(1)–F(5)	–	90.014
	F(3)–Co(1)–F(6)	–	179.996
	F(3)–Co(1)–F(7)	–	90.000
	F(4)–Co(1)–F(5)	–	180.000
	F(4)–Co(1)–F(6)	–	90.010
	F(4)–Co(1)–F(7)	–	90.010
	F(5)–Co(1)–F(6)	–	89.990
	F(5)–Co(1)–F(7)	–	89.990
	F(6)–Co(1)–F(7)	–	90.000

*See Fig. 1 for more details

reported in Table 3. We can view the metal t_{2g} orbitals are now slightly antibonding (π^*) therefore it is less energetically favourable to fill them. Note the effect on the t_{2g} d-orbitals in comparison to the σ-only case. These t_{2g} orbitals have risen in energy, closer to the, e.g., level, resulting in a reduction of Δ_{oct}. In the NBO analysis, in order to compute the span of the valence space, each sigma bonding (σ_{AB}), must in turn, be paired with a anti bonding (σ^*_{AB}): Namely, the Lewis σ-type (donor) are complemented by the non-Lewis σ^*-type (acceptor) NBO that are formally empty in an idealized Lewis structure picture. Readily, the general transformation to NBO leads to orbitals that are unoccupied in the formal Lewis structure. So, second order perturbation theory analysis of fock matrix in NBO basis at the level of B3LYP theory and EPR-II basis set for F atom and Def2-TZVP basis set and Stuttgart RSC 1997 ECP for Co (III) have been reported in Table 4 and second order perturbation theory analysis of fock matrix in NBO basis at the level of B3LYP theory and EPR-II basis set for B,N,F atoms and Def2-TZVP basis set and Stuttgart RSC 1997 ECP for Co (III) in Loop 1-$[CoF_6]^{3-}$, Loop 2-$[CoF_6]^{3-}$ and Loop 5-$[CoF_6]^{3-}$ system have been reported in Tables 5, 6 and 7. Natural bond orbital (NBO) analysis of the $[CoF_6]^{3-}$ complex at the level of B3LYP theory and EPR-II basis set for F atom and Def2-TZVP basis set and Stuttgart RSC 1997 ECP for Co (III) has been given in Table 8. The coefficients of s,p and d orbitals of (Co-F) bond, LP*(Co) and LP (F) as well as the hybridization of atoms can be distinguished based on these NBO data. It has been found that the bonding and

Table 2 Natural atomic orbitals of $[CoF_6]^{3-}$ complex with six π-donor ligands

Natural atomic orbital			
Atom	$[CoF_6]^{3-}$		
	Atomic Orbital	Energy	Occ
$Co^{3+}(1)$	4s	1.76518	0.19246
	$3d_z2$	0.31605	1.24526
	$3d_{yz}$	0.30758	1.11468
	$3d_{xy}$	0.30339	1.14252
	$3d_x2_y2$	0.26531	1.3111
	$3d_{xz}$	0.18725	1.99803
F(2)	2s	−1.34343	1.98755
	$2p_x$	0.36652	1.99931
	$2p_y$	0.36655	1.97143
	$2p_z$	0.33919	1.88611
F(3)	2s	−1.34339	1.98752
	$2p_x$	0.33919	1.88945
	$2p_y$	0.36667	1.97279
	$2p_z$	0.36671	1.99933
F(4)	2s	−1.45052	1.98268
	$2p_x$	0.31336	1.95806
	$2p_y$	0.27353	1.86189
	$2p_z$	0.31301	1.96083
F(5)	2s	−1.44774	1.98269
	$2p_x$	0.31667	1.94817
	$2p_y$	0.27478	1.86758
	$2p_z$	0.31497	1.96272
F(6)	2s	−1.34322	1.98752
	2px	0.33932	1.88922
	$2p_y$	0.3668	1.97274
	$2p_z$	0.36684	1.99933
F(7)	2s	−1.34343	1.98755
	$2p_x$	0.36652	1.99931
	$2p_y$	0.36655	1.97143
	$2p_z$	0.33919	1.88611

anti-bonding coefficients of s, p and d orbitals of Co–F bonds were 0.3 and 0.9 respectively. Based on the constant values of the coefficients of linear combination of s and p orbitals of different bonds (0.9 and 0.3), a specific voltage differences could be expected. Bond orbital, Coefficients and Hybrids of $[CoF_6]^{3-}$ complex at the level of B3LYP theory and EPR-II basis set for F atom and Def2-TZVP basis set and Stuttgart RSC 1997 ECP for Co (III) have been reported in Table 8. For further to determination non-bonded interaction of the $[CoF_6]^{3-}$ complex embedded in nano ring, we focus on the single wall boron-nitride an armchair $B_{18}N_{18}$ nanotube with chirality $n = m = 6$, and the schematic of optimized structure of the

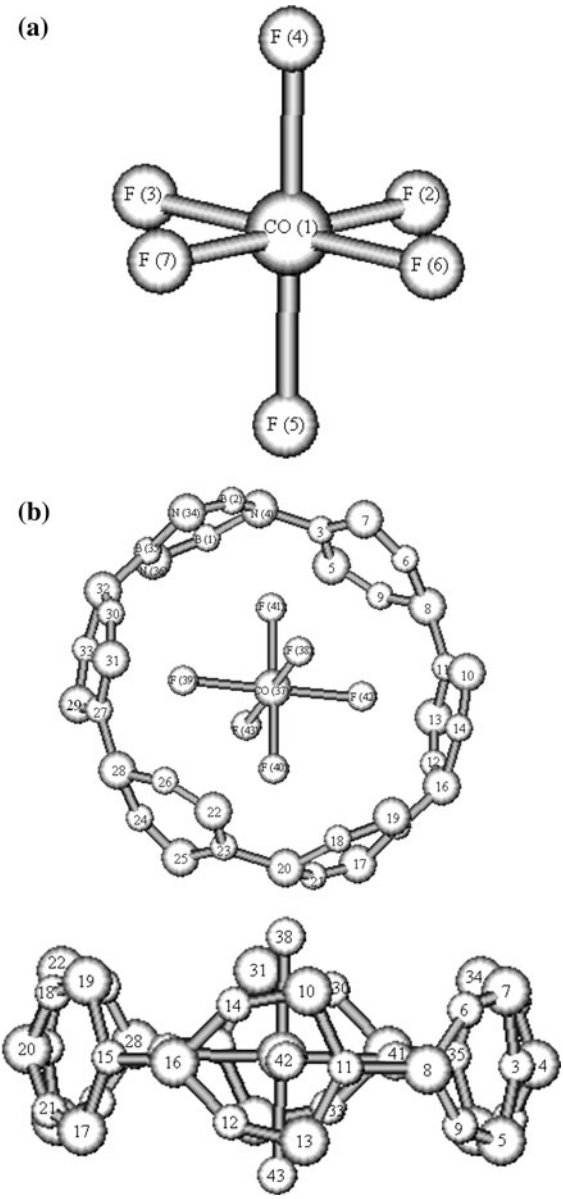

Fig. 1 The optimized geometrical structure of the **a** $[CoF6]^{3-}$ complex and **b** $B_{18}N_{18}$-$[CoF6]^{3-}$ system at the level of B3LYP/EPR-III theory

$B_{18}N_{18}$-$[CoF_6]^{3-}$ system have been displayed in Fig. 1. The geometry of $B_{18}N_{18}$ nano ring has been optimized by B3LYP method with EPR-II basis set. The Gaussian quantum chemistry package is used for all calculations. Vibration frequencies have been calculated at the level of B3LYP/EPR-II theory to verify that the geometry was a real minimum without any imaginary frequency and analyze the

Table 3 Molecular orbital diagram of $[CoF_6]^{3-}$ complex with six π-donor ligands

Compound	Molecular orbital diagram			
	Natural bond orbitals		Energy (a.u.)	Occupancy
$[CoF_6]^{3-}$	BD*(1)Co1–F4	σ^*_{t1u}	0.56761	0.13585
	BD*(1)Co1–F3	σ^*_{a1g}	0.54690	0.11162
	BD*(1)Co1–F2	$\sigma^*_{e.g}$	0.54612	0.11537
	LP*(3)Co1	π^*_{t2g}	0.31682	0.13056
	LP*(2)Co1	σ^*_{t1u}	0.31164	0.14524
	LP(3)F7	n.b.	0.18824	0.99969
	LP(3)F2	n.b.	0.18824	0.99969
	LP(3)F6	n.b.	0.18793	0.99969
	LP(3)F3	n.b.	0.18787	0.99969
	LP(1)F6	n.b.	0.18519	0.99971
	LP(1)F3	n.b.	0.18513	0.99971
	LP(1)F7	n.b.	0.18513	0.99971
	LP(1)F2	n.b.	0.18513	0.99971
	LP(3)F5	n.b.	0.16829	0.99962
	LP(3)F4	n.b.	0.16451	0.99962
	LP(2)F5	n.b.	0.16438	0.99963
	LP(2)F4	n.b.	0.16386	0.99963
	LP(1)Co1	π_{t2g}	0.13537	0.99949
	BD(1)Co1–F2	σ_{t1u}	0.07407	0.99240
	BD(1)Co1–F3	$\sigma_{e.g}$	0.07110	0.99322
	BD(1)Co1–F4	σ_{a1g}	0.02385	0.98355
	Δ_{oct}	0.2293 a.u.		

thermo chemical functions including enthalpies and Gibbs free energies [37]. According to the frequency calculation at the level of B3LYP/EPR-II theory, obtaining thermo chemical functions such as $\Delta G = -67.7929$ kcal/mol and $\Delta H = -124.4012$ kcal/mol confirmed the structural stability of $B_{18}N_{18}$ nano ring. This effect is probably due to the large dipole moments of the B–N bonds, which preferentially enhance the ring stability. The geometry of $B_{18}N_{18}$ nano-ring and $[CoF_6]^{3-}$ have been optimized by B3LYP method with EPR-II basis set for B,N,F atoms and Def2-TZVP basis set and Stuttgart RSC 1997 ECP for Co (III). The electron paramagnetic resonance (EPR) spectra and the paramagnetic parameters derived therefrom provide stringent tests of quantitative molecular orbital calculations. So it is notable that the obtained energy of mentioned basis set and ECP for $B_{18}N_{18}$ nano- ring and $[CoF_6]^{3-}$ were -1434.1167014 and -743.7823343 (Hartree) respectively. To investigate the non-bonded interaction on $[CoF_6]^{3-}$ with six different segments including six loops and six connecting bonds of $B_{18}N_{18}$ nano ring, first the six hexagon loops have been freezed and the electrostatic interaction of $[CoF_6]^{3-}$ with the one remained active loop have been considered. Other loops have been examined one by one in the same way and the changes of all the following calculated quantities have been explored. Next, we were focused on each

Table 4 Second order perturbation theory analysis of fock matrix in NBO basis at the level of B3LYP theory and EPR-II basis set for F atom and Def2-TZVP basis set and Stuttgart RSC 1997 effective core potential for Co (III)

Compound	Natural bond orbital (NBO) analysis				
	Donor NBO (i)	Acceptor NBO (j)	E(2) kcal/mol	E(j)–E(i) a.u.	F(i,j) a.u.
$[CoF_6]^{3-}$	BD(1)Co1–F2	BD*(1)Co1–F3	0.38	0.47	0.018
	BD(1)Co1–F2	BD*(1)Co1–F4	1.05	0.49	0.031
	BD(1)Co1–F3	BD*(1)Co1–F2	0.32	0.48	0.017
	BD(1)Co1–F3	BD*(1)Co1–F4	0.90	0.50	0.029
	BD(1)Co1–F4	BD*(1)Co1–F2	2.40	0.52	0.047
	BD(1)Co1–F4	BD*(1)Co1–F3	2.30	0.52	0.046
	BD(1)Co1–F4	BD*(1)Co1–F4	0.30	0.54	0.017
	LP(2)F2	BD*(1)Co1–F4	0.26	1.17	0.024
	LP(3)F2	LP*(3)Co1	3.94	0.13	0.030
	LP(3)F3	LP*(2)Co1	3.90	0.12	0.030
	LP(1)F4	BD*(1)Co1–F2	0.27	1.20	0.024
	LP(1)F4	BD*(1)Co1–F3	0.27	1.20	0.024
	LP(1)F4	BD*(1)Co1–F4	0.26	1.22	0.024
	LP(2)F4	LP*(3)Co1	5.71	0.15	0.039
	LP(3)F4	LP*(2)Co1	5.92	0.15	0.039
	BD*(1)Co1–F2	BD*(1)Co1–F4	373.21	0.02	0.226
	BD*(1)Co1–F3	BD*(1)Co1–F4	372.92	0.02	0.223
	LP(2)F5	LP*(3)Co1	5.55	0.15	0.039
	LP(3)F5	LP*(2)Co1	6.70	0.14	0.041
	LP(3)F6	LP*(2)Co1	3.88	0.12	0.029
	LP(3)F7	LP*(3)Co1	3.94	0.13	0.030
	LP(3)F7	LP*(3)Co1	3.94	0.13	0.030

bond of $B_{18}N_{18}$ individually and evaluated the interaction of $[CoF_6]^{3-}$ with each six connecting bonds of $B_{18}N_{18}$ ring and repeated the calculations along each bond. So, Total atomic charges, spin densities, and isotropic fermi coupling constants of $[CoF_6]^{3-}$ under different loops and bonds of $B_{18}N_{18}$ system at the level of B3LYP theory and EPR-II basis set for B,N,F atoms and Def2-TZVP basis set and Stuttgart RSC 1997 ECP for Co (III) have been reported in Table 9.

In accordance with Fig. 1b, it is demonstrated that atoms F(42) and F(39) are exactly in central direction of loop 3, loop 6 and between F(42) atom of the complex and N(16) of loop3 and between F(39) and N(32) atoms of loop 6 that N and F atoms are both Lewis base, non bonded interaction is existed; loop 3 and loop 6 are consisted of two π bonds. F(41) atom cooperates non bonded interaction as an Lewis acid with B(3) atom of loop 2 and F(40) atom that is against to F(41) as an Lewis acid, cooperates non bonded interaction with B(23) atom; loop 2 and loop 5 have both four π-bonds. F(38) and F(43) atoms that are out of $B_{18}N_{18}$ nano ring fields, have no non bonded interaction with nano ring. In addition, F(39) atom has non bonded interaction with B(35) too, and loop 1, has two π-bonds and loop 4 that is

Table 5 Second order perturbation theory analysis of fock matrix in NBO basis at the level of B3LYP theory and EPR-II basis set for B,N,F atoms and Def2-TZVP basis set and Stuttgart RSC 1997 ECP for Co (III) in Loop 1-$[CoF_6]^{3-}$ system

Compound	Natural bond orbital (NBO) analysis				
	Donor NBO (i)	Acceptor NBO (j)	E(2) kcal/mol	E(j)–E(i) a.u.	F(i,j) a.u.
Loop 1-$[CoF_6]^{3-}$	BD(1)B35–F39	LP*(2)Co37	0.05	0.20	0.004
	BD(1)B35–F39	LP*(3)Co37	0.46	0.21	0.013
	BD(1)B35–F39	BD*(1)Co37–F38	1.56	0.40	0.032
	BD(1)B35–F39	BD*(1)Co37–F40	1.25	0.40	0.029
	BD(1)B35–F39	BD*(1)Co37–F42	22.94	0.38	0.119
	LP(2)F39	LP*(2)Co37	1.45	0.15	0.020
	LP(3)F39	LP*(3)Co37	2.00	0.19	0.025
	LP(3)F39	BD*(1)Co37–F38	0.11	0.38	0.009
	LP(3)F39	BD*(1)Co37–F40	0.41	0.37	0.016
	LP(3)F39	BD*(1)Co37–F42	2.83	0.36	0.042
	BD(1)Co37–F38	BD*(1)Co37–F40	0.86	0.43	0.026
	BD(1)Co37–F38	BD*(1)Co37–F42	0.64	0.42	0.022
	BD(1)Co37–F40	BD*(1)Co37–F38	1.11	0.48	0.031
	BD(1)Co37–F40	BD*(1)Co37–F42	1.42	0.47	0.034
	BD(1)Co37–F42	BD*(1)Co37–F38	0.90	0.43	0.026
	BD(1)Co37–F42	BD*(1)Co37–F40	1.51	0.43	0.034
	LP*(3)Co37	BD*(1)Co37–F38	0.44	0.19	0.023
	LP*(3)Co37	BD*(1)Co37–F40	0.27	0.18	0.018
	LP(3)F38	LP*(2)Co37	4.34	0.12	0.031
	LP(2)F40	LP*(2)Co37	3.57	0.14	0.030
	LP(3)F40	LP*(3)Co37	6.14	0.15	0.040
	LP(2)F42	LP*(2)Co37	1.65	0.13	0.020
	LP(3)F42	LP*(3)Co37	3.71	0.14	0.030
	BD*(1)Co37–F42	BD*(1)Co37–F38	197.95	0.02	0.159
	BD*(1)Co37–F42	BD*(1)Co37–F40	340.00	0.01	0.174
	LP(3)F41	BD*(1)B35–F39	0.03	0.15	0.003
	LP(2)F41	LP*(2)Co37	2.99	0.17	0.030
	LP(3)F41	LP*(3)Co37	4.42	0.18	0.037
	LP(3)F41	BD*(1)Co37–F40	0.16	0.37	0.010
	LP(3)F41	BD*(1)Co37–F42	0.12	0.35	0.008
	LP(3)F43	LP*(2)Co37	4.18	0.12	0.030
	LP(3)F43	BD*(1)Co37–F38	0.08	0.32	0.007
	LP(3)F43	BD*(1)Co37–F40	0.04	0.32	0.005
	LP(3)F43	BD*(1)Co37–F42	0.03	0.31	0.004

exactly against to loop 1 has no non bonded interaction with F atoms of complex CoF_6^{3-}, and loop 4 has three decussate π-bonds (Table 9). The different energy levels of metal-ligands bonding in B_{18}-N_{18}-$[CoF_6]^{3-}$ system under three different

Table 6 Second order perturbation theory analysis of fock matrix in NBO basis at the level of B3LYP theory and EPR-II basis set for B,N,F atoms and Def2-TZVP basis set and Stuttgart RSC 1997 ECP for Co (III) in Loop 2-$[CoF_6]^{3-}$ system

Compound	Natural bond orbital (NBO) analysis				
	Donor NBO (i)	Acceptor NBO (j)	E(2) kcal/mol	E(j)-E(i) a.u.	F(i,j) a.u.
Loop 2-$[CoF_6]^{3-}$	LP(2)F41	BD*(1)Co37–F39	0.36	1.06	0.026
	LP(2)F41	BD*(1)Co37–F40	7.79	1.07	0.120
	LP(2)F41	BD*(1)Co37–F43	0.55	1.06	0.033
	LP(3)F41	LP*(2)Co37	1.02	0.17	0.018
	LP(3)F41	LP*(3)Co37	3.59	0.17	0.033
	BD(1)Co37–F39	BD*(1)B 3–F41	0.13	0.29	0.008
	BD(1)Co37–F40	BD*(1)B 3–F41	0.17	0.32	0.010
	LP(1)F39	BD*(1)B 3–F41	0.06	0.20	0.005
	LP(3)F43	BD*(1)B 3–F41	0.04	0.18	0.004
	BD(1)Co37–F39	BD*(1)Co37–F40	0.32	0.44	0.016
	BD(1)Co37–F39	BD*(1)Co37–F43	0.66	0.43	0.023
	BD(1)Co37–F40	BD*(1)Co37–F39	0.28	0.46	0.015
	BD(1)Co37–F40	BD*(1)Co37–F43	0.83	0.46	0.027
	BD(1)Co37–F43	BD*(1)Co37–F39	2.43	0.41	0.042
	BD(1)Co37–F43	BD*(1)Co37–F40	2.90	0.42	0.046
	LP(3)F39	LP*(2)Co37	3.84	0.12	0.028
	LP(3)F39	LP*(3)Co37	1.05	0.12	0.015
	LP(3)F40	LP*(2)Co37	1.67	0.12	0.019
	LP(3)F40	LP*(3)Co37	5.71	0.13	0.036
	LP(2)F43	LP*(2)Co37	0.79	0.13	0.013
	LP(2)F43	LP*(3)Co37	3.07	0.13	0.027
	LP(3)F43	LP*(2)Co37	3.28	0.12	0.027
	LP(3)F43	LP*(3)Co37	0.79	0.13	0.013
	LP(3)F38	BD*(1)B 3–F41	0.04	0.18	0.004
	LP(2)F38	LP*(2)Co37	0.77	0.13	0.013
	LP(2)F38	LP*(3)Co37	3.08	0.13	0.027
	LP(3)F38	LP*(2)Co37	3.27	0.12	0.027
	LP(3)F38	LP*(3)Co37	0.79	0.13	0.013
	LP(2)F42	BD*(1)B 3–F41	0.09	0.21	0.006
	LP(2)F42	BD*(1)Co37–F39	1.01	0.35	0.025
	LP(2)F42	BD*(1)Co37–F40	0.15	0.36	0.010
	LP(2)F42	BD*(1)Co37—F43	0.12	0.35	0.009
	LP(3)F42	LP*(2)Co37	4.44	0.11	0.029
	LP(3)F42	LP*(3)Co37	1.22	0.12	0.016

loops have been reported in Table 10. As a check on the quality of the calculated geometrical parameters and their stability with respect to the level of theory, the HOMO and the LUMO differences have been explored. The HOMO corresponds to

Table 7 Second order perturbation theory analysis of fock matrix in NBO basis at the level of B3LYP theory and EPR-II basis set for B,N,F atoms and Def2-TZVP basis set and Stuttgart RSC 1997 ECP for Co (III) in Loop 5-$[CoF_6]^{3-}$ system

Compound	Natural bond orbital (NBO) analysis				
	Donor NBO (i)	Acceptor NBO (j)	E(2) kcal/mol	E(j)-E(i) a.u.	F(i,j) a.u.
Loop 5-$[CoF_6]^{3-}$	LP(2) F40	BD*(1)Co37–F39	0.33	1.07	0.025
	LP(2)F40	BD*(1)Co37–F41	8.44	1.06	0.124
	LP(2)F40	BD*(1)Co37–F43	0.60	1.05	0.034
	LP(3)F40	LP*(2)Co37	0.22	0.17	0.008
	LP(3)F40	LP*(3)Co37	4.41	0.18	0.037
	BD(1)Co37–F39	BD*(1)B23–F40	0.11	0.27	0.007
	BD(1)Co37–F41	BD*(1)B23–F40	0.20	0.31	0.011
	BD(1)Co37–F43	BD*(1)B23–F40	0.19	0.26	0.010
	LP(2)F39	BD*(1)B23–F40	0.12	0.17	0.006
	LP(2)F43	BD*(1)B23–F40	0.05	0.16	0.004
	BD(1)Co37–F39	BD*(1)Co37–F41	0.50	0.44	0.020
	BD(1)Co37–F39	BD*(1)Co37–F43	0.98	0.43	0.028
	BD(1)Co37–F41	BD*(1)Co37–F39	0.35	0.48	0.017
	BD(1)Co37–F41	BD*(1)Co37–F43	0.88	0.47	0.028
	BD(1)Co37–F43	BD*(1)Co37–F39	2.38	0.44	0.043
	BD(1)Co37–F43	BD*(1)Co37–F41	2.83	0.44	0.046
	BD(1)Co37–F43	BD*(1)Co37–F43	0.28	0.43	0.015
	LP(3)F39	LP*(2)Co37	4.92	0.12	0.032
	LP(3)F39	LP*(3)Co37	0.27	0.12	0.008
	LP(3)F41	LP*(2)Co37	0.37	0.13	0.009
	LP(3)F41	LP*(3)Co37	7.03	0.13	0.040
	LP(2)F43	LP*(3)Co37	3.65	0.13	0.030
	LP(3)F43	LP*(2)Co37	3.81	0.13	0.030
	BD*(1)Co37–F43	BD*(1)Co37–F39	380.90	0.02	0.192
	LP(2)F38	BD*(1)B23–F40	0.05	0.16	0.004
	LP(2)F38	LP*(2)Co37	0.16	0.13	0.006
	LP(2)F38	LP*(3)Co37	3.66	0.13	0.030
	LP(2)F38	BD*(1)Co37–F41	0.03	0.34	0.004
	LP(3)F38	LP*(2)Co37	3.78	0.13	0.030
	LP(3)F38	LP*(3)Co37	0.16	0.13	0.006
	LP(1)F42	BD*(1)B23–F40	0.07	0.16	0.005
	LP(3)F42	LP*(2)Co37	4.43	0.12	0.031
	LP(3)F42	LP*(3)Co37	0.22	0.12	0.007

a combination of lone-pair orbitals on the N atoms as well as LUMO which is characterized by large contributions from vacant p orbitals on B atoms with some admixture of N-based orbitals have been calculate. For further structural information, the lowest unoccupied molecular orbital and the highest occupied molecular

Table 8 Natural bond orbital (NBO) analysis: Bond orbital/Coefficients/Hybrids of $[CoF_6]^{3-}$ at the level of B3LYP theory and EPR-II basis set for F atom and Def2-TZVP basis set and Stuttgart RSC 1997 effective core potential for Co (III)

Compound	Natural bond orbital (NBO) analysis	
	Bond orbital	Coefficients/Hybrids
$[CoF_6]^{3-}$	BD(1)Co1–F2	$0.3386*Co1(sp^{0.04}d^{2.20}) + 0.9409*F2(sp^{13.79})$
	BD(1)Co1–F3	$0.3334*Co1(sp^{0.04}d^{2.22}) + 0.9428*F3(sp^{13.18})$
	BD(1)Co1–F4	$0.3697*Co1(sp^{0.03}d^{1.73}) + 0.9292*F4(sp^{12.96})$
	LP(1)Co1	$(sp^{0.00}d^{1.00})$
	LP*(2)Co1	$(sp^{0.01}d^{99.99})$
	LP*(3)Co1	$(sp^{0.00}d^{1.00})$
	LP(1)F2	$(sp^{1.00})$
	LP(3)F2	$(sp^{1.00})$
	LP(1)F3	$(sp^{1.00})$
	LP(3)F3	$(sp^{1.00})$
	LP(2)F4	$(sp^{1.00})$
	LP(3)F4	$(sp^{1.00})$
	LP(2)F5	$(sp^{1.00})$
	LP(3)F5	$(sp^{1.00})$
	LP(1)F6	$(sp^{1.00})$
	LP(3)F6	$(sp^{1.00})$
	LP(1)F7	$(sp^{1.00})$
	LP(3)F7	$(sp^{1.00})$
	BD*(1)Co1–F2	$0.9409*Co1(sp^{0.04}d^{2.20}) - 0.3386*F2(sp^{13.79})$
	BD*(1)Co1–F3	$0.9428*Co1(sp^{0.04}d^{2.22}) - 0.3334*F3(sp^{13.18})$
	BD*(1)Co1–F4	$0.9292*Co1(sp^{0.03}d^{1.73}) - 0.3697*F4(sp^{12.96})$

Table 9 Different quantities of $[CoF6]^{3-}$ under different loops and bonds of $B_{18}N_{18}$ system at the level of B3LYP theory and EPR-II basis set for B,N,F atoms and Def2-TZVP basis set and Stuttgart RSC 1997 effective core potential for Co (III)

Compound		Basis sets of Co (III)						
$B_{18}N_{18}$-$[CoF_6]^{3-}$		Def2-TZVP, Stuttgart RSC 1997 ECP						
		Bond ID	Bond length (Å)	Bond order	Total atomic charges	Total atomic spin densities	Isotropic fermi coupling MHz	Dipole orientation θ φ
Loop 1	B(1)	r_{1-4}	1.413974	1	−0.0147	0.000482	−0.02005	90.0
	B(2)	r_{4-2}	1.413974	1	−0.0147	0.000482	−0.02005	78.3841
	N(4)	r_{2-34}	1.293131	2	−0.2045	0.002077	0.74944	
	N(34)	r_{1-36}	1.293131	2	−0.0560	−0.00043	−0.04480	
	B(35)	r_{35-36}	1.459328	1	0.00498	−0.00221	0.10523	
	N(36)	r_{34-35}	1.459328	1	−0.0560	−0.00043	−0.04480	

Table 9 continued

Compound		Basis sets of Co (III)						
$B_{18}N_{18}$-$[CoF_6]^{3-}$		Def2-TZVP, Stuttgart RSC 1997 ECP						
		Bond ID	Bond length (Å)	Bond order	Total atomic charges	Total atomic spin densities	Isotropic fermi coupling MHz	Dipole orientation θ φ
Bond1	B(3)	r_{3-4}	1.492004	1	−0.1742	0.701884	145.7426	90.0
	N(4)				−0.2476	−0.50058	−8.87115	89.3726
Loop 2	B(3)	r_{3-5}	1.459388	2	−0.0612	0.128319	21.72458	90.0
	N(5)	r_{3-7}	1.459388	2	−0.0577	−0.00816	4.53021	134.1474
	B(6)	r_{5-9}	1.293055	2	−0.0107	0.020216	5.62525	
	N(7)	r_{6-7}	1.293055	2	−0.0577	−0.00816	4.53021	
	N(8)	r_{8-9}	1.413975	1	−0.1872	0.000635	−0.54826	
	B(9)	r_{6-8}	1.413975	1	−0.0107	0.020216	5.62525	
Bond2	N(8)	r_{8-11}	1.492148	1	−0.3675	0.749001	3.70693	90.0
	B(11)				−0.2672	0.027679	5.38088	153.4938
Loop 3	N(10)	r_{11-13}	1.459442	1	−0.1211	0.117485	24.71548	90.0
	B(11)	r_{11-10}	1.459442	1	−0.2008	0.660697	151.6903	179.6831
	B(12)	r_{12-13}	1.293060	2	−0.0749	0.076154	38.72004	
	N(13)	r_{10-14}	1.293060	2	−0.1211	0.117485	24.71548	
	B(14)	r_{12-16}	1.413930	1	−0.0749	0.076154	38.72004	
	N(16)	r_{14-16}	1.413930	1	−0.2682	0.316657	10.38782	
Bond3	B(15)	r_{15-16}	1.491968	1	−0.1976	0.728356	119.0673	90.0
	N(16)				−0.2151	0.909943	2.37329	145.3154
Loop 4	B(15)	r_{15-17}	1.459328	2	0.00472	−0.00264	−0.09924	90.0
	N(17)	r_{15-19}	1.459328	1	−0.0558	−0.00054	−0.09082	101.4969
	B(18)	r_{17-21}	1.293131	1	−0.0147	0.000314	−0.06153	
	N(19)	r_{18-19}	1.293131	2	−0.0558	−0.00054	−0.09082	
	N(20)	r_{18-20}	1.413974	1	−0.2045	0.002317	0.71227	
	B(21)	r_{20-21}	1.413974	2	−0.0147	0.000314	−0.06153	
Bond4	N(20)	r_{20-23}	1.492004		−0.2484	−0.49697	−8.85807	90.0
	B(23)				−0.1750	0.702430	145.6761	90.5899
Loop 5	N(22)	r_{22-23}	1.459388	2	−0.0525	0.000928	2.33986	90.0
	B(23)	r_{23-25}	1.459388	2	−0.0486	0.055562	8.96248	43.8833
	B(24)	r_{22-26}	1.293055	2	−0.0072	0.005769	2.27783	
	N(25)	r_{24-25}	1.293055	2	−0.0525	0.000928	2.33986	
	B(26)	r_{26-28}	1.413975	1	−0.0072	0.005769	2.27783	
	N(28)	r_{24-28}	1.413975	1	−0.1758	0.003718	−0.00196	
Bond5	B(27)	r_{27-28}	1.492148	1	−0.0194	0.449654	56.78421	90.0
	N(28)				0.49895	0.477640	0.77829	158.7584

Table 9 continued

Compound		Basis sets of Co (III)						
$B_{18}N_{18}$-$[CoF_6]^{3-}$		Def2-TZVP, Stuttgart RSC 1997 ECP						
		Bond ID	Bond length (Å)	Bond order	Total atomic charges	Total atomic spin densities	Isotropic fermi coupling MHz	Dipole orientation θ φ
Loop 6	B(27)	r_{27-31}	1.459442	1	−0.1995	0.656312	150.4633	90.0
	N(29)	r_{27-29}	1.459442	1	−0.1217	0.115522	24.52702	0.50099
	B(30)	r_{30-31}	1.293060	2	−0.0753	0.075448	38.40351	
	N(31)	r_{29-33}	1.293060	2	−0.1217	0.115522	24.52702	
	N(32)	r_{30-32}	1.413930	1	−0.2684	0.312433	10.28485	
	B(33)	r_{32-33}	1.413930	1	−0.0753	0.075448	38.40351	
Bond6	N(32)	r_{32-35}	1.491968	1	−0.2151	0.910001	2.37307	90.0
	B(35)				−0.1975	0.728384	119.0763	34.6964

Table 10 Molecular orbital diagrams of $B_{18}N_{18}$-$[CoF_6]^{3-}$ complex at the level of B3LYP theory and EPR-II basis set for B,N,F atoms and Def2-TZVP basis set and Stuttgart RSC 1997 ECP for Co (III)

Loop 1		Loop 2		Loop 5	
Natural bond orbitals	Energy (a.u.)	Natural bond orbitals	Energy (a.u.)	Natural bond orbitals	Energy (a.u.)
BD*(1)Co37–F38	0.48593	BD*(1)Co37–F40	0.46672	BD*(1)Co37–F39	0.49034
BD*(1)Co37–F40	0.48057	BD*(1)Co37–F43	0.45776	BD*(1)Co37–F41	0.48451
BD*(1)Co37–F42	0.46740	BD*(1)Co37–F39	0.45734	BD*(1)Co37–F43	0.47456
LP*(3)Co37	0.29613	LP*(3)Co37	0.27152	LP*(3)Co37	0.27947
LP*(2)Co37	0.28513	LP*(2)Co37	0.26640	LP*(2)Co37	0.27831
LP(3)F38	0.16111	LP(2)F41	0.15587	LP(2)F40	0.15825
LP(3)F43	0.16111	LP(3)F42	0.15575	LP(3)F42	0.15811
LP(1)F38	0.15703	LP(3)F39	0.15035	LP(3)F39	0.15788
LP(1)F43	0.15703	LP(3)F40	0.14238	LP(1)F42	0.15162
LP(3)F42	0.15562	LP(3)F38	0.14157	LP(3)F41	0.15062
LP(2)F42	0.15498	LP(3)F43	0.14157	LP(3)F43	0.14652
LP(3)F40	0.14245	LP(2)F43	0.14074	LP(3)F38	0.14652
LP(2)F40	0.14021	LP(2)F38	0.14074	LP(2)F43	0.14597
LP(2)F39	0.13484	LP(1)F40	0.13297	LP(2)F38	0.14597
LP(2)F41	0.12005	LP(1)F39	0.11946	LP(2)F39	0.13791
LP(3)F41	0.11429	LP(2)F42	0.10999	LP(1)F41	0.13027
LP(3)F39	0.10644	LP(3)F41	0.09838	LP(3)F40	0.10396

Table 10 continued

Loop 1		Loop 2		Loop 5	
Natural bond orbitals	Energy (a.u.)	Natural bond orbitals	Energy (a.u.)	Natural bond orbitals	Energy (a.u.)
LP(1)Co37	0.10413	LP(1)Co37	0.09003	LP(1)Co37	0.10092
BD(1)Co37–F42	0.05458	BD(1)Co37–F43	0.04480	BD(1)Co37–F43	0.04850
BD(1)Co37–F38	0.04854	BD(1)Co37–F39	0.03119	BD(1)Co37–F39	0.04510
BD(1)Co37–F40	0.00176	BD(1)Co37–F40	−0.00414	BD(1)Co37–F41	0.00563
Δ_{oct}	0.17127	Δ_{oct}	0.18582	Δ_{oct}	0.19509

Table 11 Relative energies (ΔE), radial coordinate of dipole moment (r) and band gap of $[CoF_6]^{3-}$ under different loops and bonds of $B_{18}N_{18}$ at EPR-II basis set for B,N,F atoms and Def2-TZVP basis set and Stuttgart RSC 1997 effective core potential for Co (III)

Compound	Basis sets for Co^{3+}			
$B_{18}N_{18}$-$[CoF_6]^3$	Def2-TZVP, Stuttgart RSC 1997 ECP			
	Band gap (Hartree)	ΔE (Hartree)	Dipole moment (Debye)	NICS
Loop 1-$[CoF_6]^{3-}$	0.03659	−982.65042	6.6680	−9.8094
Bond 1-$[CoF_6]^{3-}$	0.08516	−823.24785	7.9548	
Loop 2-$[CoF_6]^{3-}$	0.04825	−982.66282	8.1198	−9.8196
Bond 2-$[CoF_6]^{3-}$	0.03138	−823.22981	13.6766	
Loop 3-$[CoF_6]^{3-}$	0.02648	−982.60022	13.0825	−9.8051
Bond 3-$[CoF_6]^{3-}$	0.07568	−823.2076	7.4861	
Loop 4-$[CoF_6]^{3-}$	0.03664	−982.65055	6.6633	−9.8094
Bond 4-$[CoF_6]^{3-}$	0.08492	−823.24791	7.9731	
Loop 5-$[CoF_6]^{3-}$	0.0441	−982.66281	7.3290	−9.8196
Bond 5-$[CoF_6]^{3-}$	0.03139	−822.69026	10.6949	
Loop 6-$[CoF_6]^{3-}$	0.02434	−982.60002	13.0791	−9.8051
Bond 6-$[CoF_6]^{3-}$	0.07569	−823.20760	7.4862	

orbital differences, namely band gaps have been reported to explore the ability of the suitable $[CoF_6]^{3-}$ forms to create a stable $B_{18}N_{18}$-$[CoF_6]^{3-}$ system. So, quantities values such as the relative energies (ΔE), radial coordinate of dipole moment (r), band gaps and NICS of $B_{18}N_{18}$-$[CoF_6]^{3-}$ system have been reported in Table 11. To justify the structural stability of various $B_{18}N_{18}$-$[CoF_6]^{3-}$ systems, the HOMO-LUMO band gap as the differences between HOMO and LUMO orbital has been found as a measure of the structural stability and semi-conducting properties for the purpose. DFT methods (particularly B3LYP) with EPR-II basis sets seemed as a suitable theoretical model for the computation of hyperfine coupling constants. Bond orbital, Coefficients and Hybrids of the Loop 1, Loop 2 and Loop 5 with $[CoF_6]^{3-}$ in $B_{18}N_{18}$-$[CoF_6]^{3-}$ system at the level of B3LYP theory and EPR-II basis set for N,B and F atoms and Def2-TZVP basis set and Stuttgart RSC 1997 ECP for Co (III) has been given in Table 12. The coefficients of s, p and d orbitals of (Co–F)

Table 12 Natural bond orbital (NBO) analysis: bond orbital/coefficients/hybrids, of Loop 1, Loop 2 and Loop 5 with $[CoF_6]^{3-}$ at the level of B3LYP theory and EPR-II basis set for F atom and Def2-TZVP basis set and Stuttgart RSC 1997 effective core potential for Co (III)

Natural bond orbital analysis								
Loop 1 $[CoF_6]^{3-}$			Loop 2 $[CoF_6]^{3-}$			Loop 5 $[CoF_6]^{3-}$		
Bond orbital	Coefficients/Hybrids	Occupancy	Bond orbital	Coefficients/Hybrids	Occupancy	Bond orbital	Coefficients/Hybrids	Occupancy
BD(1)Co37–F38	$0.3455*Co37(sp^{0.04}d^{2.11})$ $+0.9384*F38(sp^{14.67})$	0.99224	BD(1)Co37–F39	$0.3397*Co37(sp^{0.04}d^{2.17})$ $+0.9405*F39(sp^{13.93})$	0.99210	BD(1)Co37–F39	$0.3485*Co37(sp^{0.05}d^{2.23})$ $+0.9373*F39(sp^{15.47})$	0.99126
BD(1)Co37–F40	$0.3711*Co37(sp^{0.02}d^{1.94})$ $+0.9286*F40(sp^{13.06})$	0.98460	BD(1)Co37–F40	$0.3678*Co37(sp^{0.03}d^{2.32})$ $+0.9299*F40(sp^{12.33})$	0.98887	BD(1)Co37–F41	$0.3672*Co37(sp^{0.03}d^{2.26})$ $+ 0.9301*F41(sp^{12.34})$	0.98823
BD(1)Co37–F42	$0.3699*Co37(sp^{0.04}d^{2.08})$ $+0.9291*F42(sp^{17.75})$	0.98799	BD(1)Co37–F43	$0.3855*Co37(sp^{0.04}d^{1.68})$ $+0.9227*F43(sp^{20.94})$	0.98069	BD(1)Co37–F43	$0.3804*Co37(sp^{0.04}d^{1.70})$ $+0.9248*F43(sp^{19.90})$	0.98191
LP(1)Co37	$(sp^{0.00}d^{1.00})$	0.99872	LP(1)Co37	$(sp^{0.00}d^{1.00})$	0.99785	LP(1)Co37	$(sp^{0.00}d^{1.00})$	0.99546
LP*(2)Co37	$(sp^{0.04}d^{99.99})$	0.13666	LP*(2)Co37	$(sp^{0.01}d^{99.99})$	0.15214	LP*(2)Co37	$(sp^{0.01}d^{99.99})$	0.14509
LP*(3)Co37	$(sp^{0.23}d^{99.99})$	0.12104	LP*(3)Co37	$(sp^{0.00}d^{1.00})$	0.13535	LP*(3)Co37	$(sp^{0.00}d^{1.00})$	0.13709
LP(1)F38	$(sp^{99.99}d^{0.06})$	0.99934	LP(2)F38	$(sp^{1.00}\ d^{0.00})$	0.97324	LP(2)F38	$(sp^{1.00}d^{0.00})$	0.97191
LP(3)F38	$(sp^{99.99}d^{0.02})$	0.96630	LP(3)F38	$(sp^{1.00}\ d^{0.00})$	0.96939	LP(3)F38	$(sp^{1.00}d^{0.00})$	0.97012
LP(2)F39	$(sp^{1.00}d^{0.00})$	0.98593	LP(1)F39	$(sp^{33.91}\ d^{0.00})$	0.99924	LP(2)F39	$(sp^{60.14}d^{0.00})$	0.98888
LP(3)F39	$(sp^{28.94}d^{0.00})$	0.94812	LP(3)F39	$(sp^{1.00}\ d^{0.00})$	0.95838	LP(3)F39	$(sp^{1.00}d^{0.00})$	0.94969
LP(2)F40	$(sp^{1.00}d^{0.00})$	0.97417	LP(1)F40	$(sp^{99.99}d^{0.01})$	0.99963	LP(2)F40	$(sp^{0.28}d^{0.00})$	0.97977
LP(3)F40	$(sp^{99.99}d^{0.03})$	0.94981	LP(3)F40	$(sp^{1.00}\ d^{0.00})$	0.94528	LP(3)F40	$(sp^{1.00}d^{0.00})$	0.96976
LP(2)F41	$(sp^{1.00}d^{0.00})$	0.96999	LP(2)F41	$(sp^{0.24}\ d^{0.00})$	0.98113	LP(1)F41	$(sp^{65.69}d^{0.00})$	0.99931
LP(3)F41	$(sp^{99.99}d^{0.00})$	0.96058	LP(3)F41	$(sp^{1.00}\ d^{0.00})$	0.97061	LP(3)F41	$(sp^{1.00}d^{0.00})$	0.94536
LP(2)F42	$(sp^{1.00}d^{0.00})$	0.98682	LP(2)F42	$(sp^{21.01}\ d^{0.00})$	0.99358	LP(1)F42	$(sp^{99.99}d^{0.01})$	0.99956
LP(3)F42	$(sp^{99.99}d^{0.01})$	0.97002	LP(3)F42	$(sp^{1.00}\ d^{0.00})$	0.94655	LP(3)F42	$(sp^{1.00}d^{0.00})$	0.96169
LP(1)F43	$(sp^{99.99}d^{0.06})$	0.99934	LP(2)F43	$(sp^{1.00}\ d^{0.00})$	0.97324	LP(2)F43	$(sp^{1.00}d^{0.00})$	0.97191
LP(3)F43	$(sp^{99.99}d^{0.02})$	0.96630	LP(3)F43	$(sp^{1.00}\ d^{0.00})$	0.96939	LP(3)F43	$(sp^{1.00}d^{0.00})$	0.97012

Table 12 continued

Natural bond orbital analysis								
Loop 1 $[CoF_6]^{3-}$			Loop 2 $[CoF_6]^{3-}$			Loop 5 $[CoF_6]^{3-}$		
Bond orbital	Coefficients/Hybrids	Occupancy	Bond orbital	Coefficients/Hybrids	Occupancy	Bond orbital	Coefficients/Hybrids	Occupancy
BD*(1)Co37–F38	$0.9384*Co37(sp^{0.04}d^{2.11})-0.3455*F38(sp^{14.67})$	0.12000	BD*(1)Co37–F39	$0.9405*Co37(sp^{0.04}d^{2.17})-0.3397*F39(sp^{13.93})$	0.12361	BD*(1)Co37–F39	$0.9373*Co37(sp^{0.05}d^{2.23})-0.3485*F39(sp^{15.47})$	0.11563
BD*(1)Co37–F40	$0.9286*Co37(sp^{0.02}d^{1.94})-0.3711*F40(sp^{13.06})$	0.12472	BD*(1)Co37–F40	$0.9299*Co37(sp^{0.03}d^{2.32})-0.3678*F40(sp^{12.33})$	0.09360	BD*(1)Co37–F41	$0.9301*Co37(sp^{0.03}d^{2.26})-0.3672*F41(sp^{12.34})$	0.09262
BD*(1)Co37–F42	$0.9291*Co37(sp^{0.04}d^{2.08})-0.3699*F42(sp^{17.75})$	0.10996	BD*(1)Co37–F43	$0.9227*Co37(sp^{0.04}d^{1.68})-0.3855*F43(sp^{20.94})$	0.14748	BD*(1)Co37–F43	$0.9248*Co37(sp^{0.04}d^{1.70})-0.3804*F43(sp^{19.90})$	0.14411

bond as well as the hybridization of atoms can be distinguished based on these NBO data. It has been found that the bonding and anti-bonding coefficients of s, p and d orbitals of Co–F bonds in different loops were 0.9 and 0.3, respectively. Based on the constant values of the coefficients of linear combination of s, p and d orbitals of different bonds (0.9 and 0.3), a specific voltage differences could be expected.

Conclusion

In this study, we used DFT methods with EPR basis sets to determination electrostatic non-bonded interaction among nano-systems. So the results of hybrid DFT with EPR quantum-chemical calculations were useful for assignment of the provided a basis for description of electromagnetic non-bonded interaction between $B_{18}N_{18}$ nano ring and $[CoF_6]^{3-}$ octahedral complex. Because of the electrostatic and hyperfine characteristics of $B_{18}N_{18}$-$[CoF_6]^{3-}$ system, those techniques dealing with electron distributions around nuclei including relative energies, HOMO-LUMO band gaps, total atomic charges, spin densities, of $[CoF_6]^{3-}$ in different loops and bonds have been employed to detect and characterize the hyperfine structural properties of $B_{18}N_{18}$-$[CoF_6]^{3-}$ system. In this study, first, we have discussed the different aspects of electronic structure of the $B_{18}N_{18}$-$[CoF_6]^{3-}$ system for further validation of theoretical results to increase there usefulness in practical applications or for pre-experimental modeling. Second, we have explored the electromagnetic nature of the $B_{18}N_{18}$-$[CoF_6]^{3-}$ system through calculating the following parameters which provide valuable information on the interaction characteristics. Also, it has been found at Tables 8 and 12 that the bonding and anti-bonding coefficients of s, p and d orbitals of Co–F bonds in $[CoF_6]^{3-}$ complex and under field effects of different loops of $B_{18}N_{18}$ nano-ring were 0.9 and 0.3. In accordance with Table 10 in comparison with Table 3, it is demonstrated that energy levels of σ bonds or bonding and σ^* or anti bonding related to Co-F under the field effect of each loops in the supposed nano ring, have become lower and more stable. In the other hand, Δ_{oct} for $[CoF_6]^{3-}$ 0.2293 a.u. and at last, field effect of loop 1, loop 2 and loop 5 of $B_{18}N_{18}$ nano ring are respectively 0.17127, 0.18582 and 0.19509; thus, Δ_{oct} has been lower because of nano ring field. In accordance with NICS values of Table 11, it's elaborated that the loops are across to each other in $B_{18}N_{18}$ nano ring, loop 1–loop 4, loop 3–loop 6 and loop 2–loop 5 have similar NICS values; it means circle currency or aromaticity of such loop 1 and loop 4 are the same and equal to −9.8094; loop 2 and loop 5 have more negative NICS values that is equal to −9.8196 so that if the NICS value would be more negative, the aromaticity and magnetism of the circle is more.

References

1. P. W. Fowler, K. M. Rogers, G. Seifert, M. Terrones, and H. Terrones (1999). *Chem. Phys. Lett.* **299**, 359.
2. Y. Liu, Z. Wenli, B. B. Isaac, and J. E. Boggs (2009). *J. Chem. Phys.* **30**, 184305.

3. A. Loiseau, F. Willaime, N. Demoncy, N. Schramchenko, and G. Hug (1998). *Carbon* **36**, 743–752.
4. M. L. Sun, Z. Slanina, and S. L. Lee (1995). *Chem. Phys. Lett.* **233**, 279.
5. M. Monajjemi, H. Aghaie, and F. Naderi (2007). *Biochemistry (Moscow)* **72**, 799.
6. O. Takeo, K. Masaki, K. Hidehiko, and N. Ichihito (2001). *Int. J. Inorg. Mater.* **3**, 597.
7. S. H. Xu, M. Y. Zhang, Y. Y. Zhao, B. G. Cheng, J. Zhang, and C. C. Sun (2006). *Chem. Phys. Lett.* **418**, 297.
8. D. L. Strout (2000). *J. Phys. Chem. A* **104**, 3364.
9. D. L. Strout (2001). *J. Phys. Chem. A* **105**, 261.
10. D. L. Strout (2004). *Chem. Phys. Lett.* **383**, 95.
11. S. S. Alexandre, M. S. C. Mazzoni, and H. Chacham (1999). *Appl. Phys. Lett.* **75**, 61.
12. S. S. Alexandre, R. W. Nunes, and H. Chacham (2002). *Phys. Rev. B* **66**, 085.
13. H. S. Wu and H. J. Jiao (2004). *Chem. Phys. Lett.* **386**, 369.
14. H. S. Wu, X. H. Xu, D. L. Strout, and H. J. Jiao (2005). *J. Mol. Model.* **12**, 1.
15. K. W. Rogers, P. W. Fowler, and G. Seifert (2000). *Chem. Phys. Lett.* **332**, 43.
16. M. Monajjemi, L. Mahdavian, and F. Mollaamin (2008). *Bull. Chem. Soc. Ethio.* **22**, 1.
17. F. Mollaamin, S. Gharibe, and M. Monajjemi (2011). *Int. J. Phys. Sci.* **6**, 1496.
18. M. Monajjemi, H. Chegini, F. Mollaamin, and P. Farahani (2011). *Fullerenes, Nanotub Carbon Nanostructure* **19**, 469.
19. F. Mollaamin, F. Najafi, M. Khaleghian, B. Khalili Hadad, and M. Monajjemi (2011). *Fullerenes, Nanotub Carbon Nanostructures* **19**, 653.
20. L. B. Knight Jr, D. W. Hill, T. J. Kirk, and C. A. Arrington (1992). *J. Phys. Chem.* **96**, 555.
21. Z. Slanina, J. M. L. Martin, J. P. Franqois, and R. Gijbels (1993). *Chem. Phys. Lett.* **201**, 54.
22. Z. Slanina, J. M. L. Martin, J. P. Franqoisand, and R. Gijbels (1993). *Chem. Phys.* **178**, 77.
23. M. Monajjemi, L. Mahdavian, F. Mollaamin, and M. Khaleghian (2009). *Rus. J. Inorg. Chem.* **54**, 1465–1473.
24. S. Iijima and T. Ichihashi (1993). *Nature* **363**, 603.
25. P. M. Ajayan (1999). *Chem. Rev.* **99**, 1787.
26. R. F. Curl and R. E. Smalley (1988). *Science* **242**, 1017.
27. H. Y. Zhu, D. J. Klein, W. A. Seitz, and N. H. March (1995). *Inorg. Chem.* **34**, 1377.
28. S. M. Glauciete and G. Edgardo (2005). *Chem. Phys. Lett.* **409**, 29.
29. D. K. Hoffman, R. Ruedenberg, and J. G. Verkade (1977). *Struct. Bond.* **33**, 57.
30. M. Monajjemi, V. S. Lee, M. Khaleghian, B. Honarparvar, and F. Mollaamin (2010). *J. Phys. Chem. C* **114**, 15315.
31. A. D. Becke (1993). *J. Chem. Phys.* **98**, 5648.
32. C. Lee, W. Yang, and R. G. Parr (1998). *Phys. Rev. B* **37**, 785.
33. D. Golberg, Y. Bando, O. Stephan, and K. Kurashima (1998). *Appl. Phys. Lett.* **73**, 2441.
34. M. J. Frisch, G. W. Trucks, H. B. Schlegel, G. E. Scuseria, M. A. Robb, J. R Cheeseman, V. G. Zakrzewski, J. A. Montgomery, Jr., R. E. Stratmann, J. C. Burant, S. Dapprich, J. M. Millam, A. D. Daniels, K. N. Kudin, M. C. Strain, O. Farkas, J. Tomasi, V. Barone, M. Cossi, R. Cammi, B. Mennucci, C. Pomelli, C. Adamo, S. Clifford, J. Ochterski, G. A. Petersson, P. Y. Ayala, Q. Cui, K. Morokuma, D. K. Malick, A. D. Rabuck, K. Raghavachari, J. B. Raghavachari, J. Cioslowski, J. V. Ortiz, A. G. Baboul, B. B. Stefanov, G. Liu, A. Liashenko, P. Piskorz, I. Komaromi, R. Gomperts, R. L. Martin, D. J. Fox, T. Keith, M. A. Al-Laham, C. Y. Peng, A. Nanayakkara, C. Gonzalez, M. Challacombe, P. M. W. Gill, B. Johnson, W. Chen, M. W. Wong, J. L. Andres, C. Gonzalez, M. Head-Gordon, E. S. Replogle, J. A. Pople (1998) Gaussian 98 Revision A.7, Gaussian, Inc., Pittsburgh.
35. K. Oku, A. Nishiwaki, I. Narita, and M. Gonda (2003). *Chem. Phys. Lett.* **380**, 620.
36. E. C. Behrman, R. K. Foehrweiser, J. R. Myers, B. R. French, and M. E. Zandler (1994). *Phys. Rev. A* **49**, R1543.
37. R. B. Zhang, T. Z. Huyskensd, A. Ceulemeans, and M. T. Nguyen (2005). *Chem. Phys.* **316**, 35.
38. J. P. Foster and F. Weinhold (1980). *J. Am. Chem. Soc.* **102**, 7211.
39. M. Monajjemi, M. T. Azad, H. H. Haeri, K. Zare, and Sh. Hamedani (2003). *J. Chem. Res.* **1**, (8), 454.
40. L. Goodman, V. Pophristic, and F. Weinhold (1999). *Acc. Chem. Res.* **32**, 983.
41. A. E. Reed and F. Weinhold (1985). *J. Am. Chem. Soc.* **107**, 1919.
42. W. K. Myers, C. P. Scholes, and D. L. Tierney (2009). *J. Am. Chem. Soc.* **9**, 131.